

1 **A quick and easy way to estimate entropy and mutual information** 2 **for neuroscience**

3 Mickael Zbili^{1,2}, Sylvain Rama^{3*}

4 ¹, Lyon Neuroscience Research Center, INSERM U1028-CNRS UMR5292-Université Claude Bernard Lyon1, Lyon,
5 France

6 ², Now in Blue Brain Project, École polytechnique fédérale de Lausanne (EPFL) Biotech Campus, Geneva,
7 Switzerland.

8 ³, UCL Queen Square Institute of Neurology, University College London, London, United Kingdom.

9 *, Correspondence: Sylvain Rama, s.rama@ucl.ac.uk

10 **Abstract**

11 Calculations of entropy of a signal or mutual information between two variables are valuable
12 analytical tools in the field of neuroscience. They can be applied to all types of data, capture
13 nonlinear interactions and are model independent. Yet the limited size and number of recordings
14 one can collect in a series of experiments makes their calculation highly prone to sampling bias.
15 Mathematical methods to overcome this so called “sampling disaster” exist, but require
16 significant expertise, great time and computational costs. As such, there is a need for a simple,
17 unbiased and computationally efficient tool for reliable entropy and mutual information
18 estimation. In this paper, we propose that application of entropy-coding compression algorithms
19 widely used in text and image compression fulfill these requirements. By simply saving the
20 signal in PNG picture format and measuring the size of the file on the hard drive, we can reliably
21 estimate entropy through different conditions. Furthermore, with some simple modifications of
22 the PNG file, we can also estimate mutual information between a stimulus and the observed
23 responses into multiple trials. We show this using White noise signals, electrophysiological
24 signals and histological data. Although this method does not give an absolute value of entropy or
25 mutual information, it is mathematically correct, and its simplicity and broad use make it a
26 powerful tool for their estimation through experiments.

27 **1 Introduction**

28 Entropy is the major component of information theory, conceptualized by Shannon in 1948
29 (Shannon, 1948). It is a dimensionless quantity representing uncertainty about the state of a
30 continuous or discrete system or a collection of data. It is highly versatile as it applies to many
31 different types of data, it can capture nonlinear interactions, and is model independent (Cover
32 and Thomas, 2006). It has been widely used in the field of neurosciences, see (Borst and
33 Theunissen, 1999; Timme and Lapish, 2018) for a more complete review of work; for example
34 in the field of synaptic transmission (London et al., 2002), information rate of Action Potentials

35 (APs) (Bialek et al., 1991; Juusola and de Polavieja, 2003; Street, 2020) or connectivity studies
36 (Ito et al., 2011; Vicente et al., 2011).

37

38 However, estimating the entropy of a signal can be a daunting task. The entropy H of a signal X
39 is calculated with the well-known Shannon's formula:

$$40 \quad H(X) = -\sum_{i=1}^N p(x_i) \log_2 p(x_i) \quad (\text{eq.1})$$

41 Where $p(x_i)$ is the probability that the signal will take the x_i configuration in the probability
42 distribution $(x_1, x_2, x_3, \dots, x_N)$ of the signal. It is considered that if $p(x_i) = 0$, then
43 $p(x_i) \log_2 p(x_i) = 0$, as $\lim_{x \rightarrow 0} x (\log_2 x) = 0$. And using a base 2 logarithm, entropy will be
44 expressed in bits (Cover and Thomas, 2006; Shannon, 1948).

45 However, correctly estimating a probability distribution works only if each configuration
46 happens many times. And by definition, one cannot know beforehand the number of needed
47 experiments. This recording bias is even amplified by the fact that without making assumptions,
48 there is no way to determine the relevant quantization and sampling of the data. The same
49 recordings could be divided in any quantization bins and sampled by any interval, all giving
50 different probability distributions and thus different entropy values.

51 As an example, let us consider the chain of characters $A="04050405"$. It is unchanged with a
52 quantization range " v " of 5, but will become "01010101" with a quantization range " v " of 2. If
53 we now sample it with a bin " T " of 1 character, this will give a probability distribution of: $p(0) =$
54 0.5 , $p(4) = p(5) = 0.25$ in the first scenario ($v = 5$) and: $p(0) = p(1) = 0.5$ in the second scenario
55 ($v = 2$). We thus obtain different entropy values in the two scenarios: $H^{v=5, T=1} = 1.5$
56 and $H^{v=2, T=1} = 1$. Now, if we take a sampling bin of $T = 2$ we obtain $p(04) = p(05) = 0.5$ for v
57 $= 5$ and $p(01) = 1$ for $v = 2$. The calculated entropies thus are: $H^{v=5, T=2} = 1$ and $H^{v=2, T=2} =$
58 0 .

59 Without making assumptions on the data, there is no way to determine which value of entropy is
60 the correct one. Therefore, quantization and sampling are crucial to determine the entropy of a
61 signal. In an ideal case, we would need a method able to correct for the sample bias without
62 making assumptions about the signal, meaning for any length of acquisition, any binning of
63 width " T " and any quantization level " v " of the recorded data.

64 Thankfully there are multiple ways to use the direct formula and compensate for this bias, but
65 none of them can be called trivial. There are for example the quadratic extrapolation method
66 (Juusola and de Polavieja, 2003; de Polavieja et al., 2005; Strong et al., 1998), the Panzeri-
67 Treves Bayesian estimation (Panzeri and Treves, 1996), the Best Universal Bound estimation
68 (Paninski, 2003), the Nemenman-Shafee-Bialek method (Nemenman et al., 2004) or some more
69 recent methods using statistic copulas (Ince et al., 2017; Safaai et al., 2018). Each method has its

70 advantages and downsides (see (Panzeri et al., 2007) for a comparison of some of them), which
71 leaves the experimenter puzzled and in dire need of a mathematician (Borst and Theunissen,
72 1999; Magri et al., 2009; Timme and Lapish, 2018).

73 However, there is another way to calculate the entropy of a signal, through what is called the
74 Source Coding Theorem (Cover and Thomas, 2006; Larsson, 1996, 1999; Shannon, 1948;
75 Wiegand, 2010) that to our knowledge has been used only once in the field of neurosciences, by
76 (London et al., 2002) to calculate the information efficacy of a given synapse.

77 In signal processing, data compression is the process of encoding information using fewer bits
78 than the original representation. In case of lossless compression, it does so by sorting parts of the
79 signal by their redundancy and replacing them by shorter code words (Huffman, 1952; Shannon,
80 1948). However, the source coding theorem specifies that it is impossible to compress a signal of
81 size N such that the length of the compressed signal is smaller than the entropy of the original
82 signal multiplied by N . Therefore, with a perfect compression method the size of the compressed
83 signal is proportional to the original signal entropy (Cover and Thomas, 2006; Larsson, 1996,
84 1999; Shannon, 1948; Wiegand, 2010).

85 When choosing this way of calculating entropy, the choice of the compression algorithm thus
86 become critical as the compressed signal must be the smallest possible in order to represent the
87 entropy of the original signal. It is of course possible to craft its own compression algorithm (see
88 (London et al., 2002)), but thankfully this application has been broadly used in the domain of
89 informatics, in order to compress text and images efficiently on the hard drive of a computer or
90 before sending data through a network. In particular, this led to the development of two principal
91 entropy-coding compression algorithms: the Huffman coding algorithm (Huffman, 1952) and the
92 the Lempel–Ziv–Storer–Szymanski algorithm (Storer and Szymanski, 1982), both used to
93 compress text and image files.

94 Portable Network Graphics (or PNG, see specifications at <https://www.w3.org/TR/PNG/> or
95 <http://www.libpng.org/pub/png/>) is a graphic file format supporting lossless data compression.
96 Its high versatility and fidelity made it widely used for saving and displaying pictures. Its lossless
97 compression is based on the combination of the Lempel–Ziv–Storer–Szymanski and Huffman
98 algorithms and is called DEFLATE (Deutsch, 1996). Its great efficacy made it a reference for
99 comparison with other entropy-encoding image compression methods (Bian et al., 2019; Cover
100 and Thomas, 2006; Hou et al., 2020; Mentzer et al., 2020) and it is even used directly to estimate
101 image entropy (Wagstaff and Corsetti, 2010).

102 In this paper, we propose that measurement of PNG file output size of neuroscientific data
103 compressed using the PNG DEFLATE algorithm (in Bytes on the hard drive) is a reliable and
104 unbiased proxy to estimate the entropy of different neuronal variables. From this simple step and
105 by applying this method to electrophysiological and histological data we show that output data
106 file size and entropy are related in a linear fashion and are robust enough to estimate entropy

107 changes in response to different conditions. Further, with minimal modifications of the PNG file,
108 we validate estimation of the mutual information between a stimulation protocol and the
109 resulting experimental recording.

110 2 Materials and Methods

111 1 Neuronal modeling

112 A single compartment model was simulated with NEURON 7.7
113 (<https://www.neuron.yale.edu/neuron/>). All simulations were run with 100- μ s time steps and had
114 duration of 5 seconds. The nominal temperature was 37°C. The voltage dependence of activation
115 and inactivation of Hodgkin-Huxley-based conductance models were taken from (Hu et al., 2009)
116 for g_{Nav} and g_{KDR} . The equilibrium potentials for Na^+ , K^+ , and passive channels were set to +60,
117 -90 and -77 mV, respectively. The conductances densities were set to 0.04 S/cm², 0.01 S/cm²
118 and $3.33 \cdot 10^{-5}$ S/cm² for g_{Nav} and g_{KDR} and passive channels, respectively. The model was
119 stimulated using various numbers of excitatory synapses using the AlphaSynapse PointProcess
120 of the NEURON software. The time constant and reversal potential were the same for every
121 synapses and were set to 0.5 ms and 0 mV, respectively. The size of EPSPs produced by the
122 synapses were randomly chosen using a lognormal distribution of EPSPs amplitude
123 experimentally described in L5 pyramidal neurons (Lefort et al., 2009). Each synapse stimulated
124 the model once during a simulation and the time onset was randomly chosen.

125 For the simulations of Figures 3A and 3B, the number of synapses simulating the model
126 depended on the spiking frequency desired. For example, to calculate the information rate in the
127 case of a 1 Hz spike train, we simulated the model with 400 of the synapses described above. We
128 ran 20 trials of the simulation with the same train of synapses (Figure 2A). In order to introduce
129 some jitter in the spiking times, we also injected a small gaussian current with a mean of 0 nA
130 and a standard deviation of 0.0005 nA during the 5 seconds of the simulation. We reproduced
131 this whole protocol for others desired spiking frequency, using increasing number of synapses
132 (for example: 1900 synapses for a 19 Hz spiking).

133 For the simulations of Figure 3C, we stimulated the model with 750 of the synapses described
134 above to get a spiking frequency around 5Hz. The time onsets and the amplitude of the synapses
135 were randomly chosen at each simulation. We also added one supplementary synapse (Syn_supp)
136 which stimulates the model every 200 ms (i.e 25 times in 5 s). The size of the EPSP size
137 produced by this synapse was called wSyn_supp. When wSyn_supp was weak, this synapse did
138 not drive the spiking of the model (Figure 3C, up left). When wSyn_supp was strong, this
139 synapse drove the spiking of the model (Figure 3C, down left). We ran 100 simulations for each
140 wSyn_supp.

141 2 Direct calculation of information rate via the quadratic extrapolation method

142 We calculated the entropy and information rates using the direct method and quadratic
143 extrapolation, as described by (Juusola and de Polavieja, 2003; Panzeri et al., 2007; de Polavieja
144 et al., 2005; Strong et al., 1998).

145 The first step of this method is to calculate the different values of entropy of the signal with
146 different portions “Size” of the signal, different quantizations “v” of the signal values and
147 different samplings bin “T”. As described in the introduction, each modification of “Size”, “v” or
148 “T” will give a different value for the entropy. For example, in figures 3A and B, the parameter
149 “Size” was successively set as 1, 0.9, 0.8, 0.7, 0.6, 0.5; “v” successively set as 2, 4, 8, 16, 32, 64,
150 128, 256 and the parameter “T” was successively set as 1, 2, 3, 4, 5, 6, 7, 8, which produced 6 *
151 8 * 8 = 384 distinct values of entropy for every trial. Entropy values for different trials of the
152 same condition were averaged together. These values were then plotted against 1/Size and the
153 intersections to 0 estimated by quadratic fit of the data. This gave us the entropy values for every
154 “v” and “T”, corrected for infinite size of the recordings. These values were then quadratic fitted
155 against 1/v. The intersection to 0 gave us entropy values for every parameters of “T”, corrected
156 for infinite Size and infinite number of bins “v”. Finally, these new values were fitted against 1/T
157 and the extrapolation to 0 was estimated, to obtain the entropy value for infinite Size of the
158 signals, infinite number of quantization levels “v” and infinite number of combination bins “T”
159 (example in Fig. 1B). By performing this triple extrapolation and dividing by the time sampling,
160 we can estimate the entropy rate R of the signal for theoretical infinite size, infinite number of
161 quantization levels and infinite combination of sampling bins as

$$R = \lim_{T \rightarrow \infty} \frac{1}{T} \lim_{T \rightarrow \infty} \lim_{T \rightarrow \infty} H^{T,v,Size}$$

162 To obtain R_N , the entropy rate of the noise, instead of calculating H along the length of the signal,
163 we did it at every time point across the successive trials. This is equivalent to simply transpose
164 the signal and re-applying the same method than for R_S . Finally, we obtained the information rate
165 by subtracting R_N to R_S as

$$R = R_S - R_N = \lim_{T \rightarrow \infty} \frac{1}{T} \lim_{v \rightarrow \infty} \lim_{Size \rightarrow \infty} (H_S^{T,v,Size} - H_N^{T,v,Size})$$

166 For Figure 3A, simulated recordings were down-sampled to 10 kHz before calculation of
167 information rate. For Figure 3C, middle, simulated recordings were down-sampled to 3 kHz and
168 binned as 0 & 1 depending of the presence of Action Potentials or not, similar to (London et al.,
169 2002).

170 For figures 1B, 1C, 1D, 2, 3A and 3B, The parameter “Size” was successively set as 1, 0.9, 0.8,
171 0.7, 0.6, 0.5; “v” successively set as 2, 4, 8, 16, 32, 64, 128, 256 and the parameter “T” was
172 successively set as 1, 2, 3, 4, 5, 6, 7, 8. For figure 3C, the parameter “Size” was successively set

173 as 1, 0.9, 0.8, 0.7, 0.6, 0.5; “v” set as 2 and the parameter “T” was successively set as 1, 2, 5, 10,
174 20, 30, 40. R_S , R_N and Information rate were calculated by successive quadratic extrapolations,
175 as described above.

176 All of this was done by custom scripts written in Python 3.7 Anaconda with Numpy, Pandas and
177 pyABF modules. These scripts are available at <https://github.com/Sylvain-Deposit/PNG-Entropy>.

178 **3 Export to PNG format**

179 Export to PNG was made with 3 different softwares: i) Anaconda 3.7
180 (<https://www.anaconda.com/>) and the pyPNG package (<https://pypi.org/project/pypng/>) for
181 Figures 1, 2A, 3A, 3B ; ii) Labview 2017 and Vision 2017 (National Instruments) for Figures
182 2B, 3C, 4A and 4B; iii) the FIJI distribution of ImageJ software (Rueden et al., 2017; Schindelin
183 et al., 2012) for figure 4C. Signals were normalized to 256 values from 0 to 255 simply by
184 subtracting the minimal value of the signal, then dividing by the maximal value and multiplying
185 by 255. It was then saved as PNG format in 8-bits range (256 grey values). For figure 2B and 3C,
186 as the signal was binnarized we saved it with a 1-bit range (2 grey values).

187 A minimal file of PNG format is composed of a header and several parts of data, named critical
188 chunks (<https://www.w3.org/TR/PNG/#5DataRep>). To these minimum requirements it is
189 possible to add ancillary chunks (<https://www.w3.org/TR/PNG/#11Ancillary-chunks>) containing
190 various information such as Software name, ICC profile, pixels dimensions, etc... If useful, this
191 is hindering the estimation of entropy as it represents an overhead to the final size of the file. To
192 estimate this overhead for each of our software we saved an image of 100 * 100 values of zeros,
193 which corresponds to black in 8-bits grey levels and has an entropy of 0. With pyPNG, Fiji and
194 Labview we obtained three PNG files of size 90, 90 and 870 Bytes, respectively. When repeating
195 the experiment of figure 1, we obtained really similar linear fits of slopes 1.21 ($R^2 = 0.99$), 1.18
196 ($R^2 = 0.99$) and 1.21 ($R^2 = 0.99$) respectively.

197 For Figure 4C, we used Fiji for every image of the collection and we: i) extracted the channel
198 number 2 containing the MAP2 staining; ii) converted the file to 8-bits grey levels; iii)
199 thresholded it to remove every intensity values under 10 to remove most of the background; iv)
200 saved the new file as PNG format, v) checked the size of this new file and vi) divided the size in
201 kBytes by the number of soma visible in the field.

202 **3 Results**

203 **1 Entropy and application to Gaussian noise**

204 To test the usability of the PNG format to represent entropy, we started by generating 10 000
205 points of uniform white noise with an amplitude N of 2. As we are using white noise, we fully
206 know the probability distribution (in that case, $p(xi) = 1/N$) and we can apply the eq. 1 and
207 obtain an entropy H of 1 bit. We then repeated this noise model progressively increasing the

208 amplitude by squares of 2 until 256, which corresponds to a maximum entropy of 8 bits (Figure
209 1A). The entropy rate R is defined as $R = \frac{1}{T}H$ with T being the sampling of the signal. In this
210 model case, we can take $T = 1$ to finally obtain an entropy rate in bits per samples.

211 As a control way to calculate the entropy of our signals, we used the quadratic extrapolation
212 method which compensate for the sampling disaster (Juusola and de Polavieja, 2003; Panzeri et
213 al., 2007; de Polavieja et al., 2005; Strong et al., 1998). Briefly, this method requires slicing our
214 signal by multiple factors “Size”, quantizing it into multiple levels “ v ” of amplitudes, creating
215 the probability distribution of words made of multiple combinations “ T ” of bins and finally
216 calculating the entropy of the signal from this probability distribution. We thus obtain a great
217 number of entropy values that we plot successively against $1/\text{Size}$, $1/v$ and $1/T$ in order to fit
218 them with quadratic extrapolations and find the intersection to 0 (Figure 1B, see Methods). By
219 this triple extrapolation, we can estimate the entropy rate of the signal for theoretical infinite size,
220 infinite quantization levels and infinite combination of sample bins as

$$221 \quad 222 \quad R = \lim_{T \rightarrow \infty} \frac{1}{T} \lim_{v \rightarrow \infty} \lim_{\text{Size} \rightarrow \infty} H^{T,v,\text{Size}} \quad (\text{eq.2})$$

223 In our simple model, we can see that when using only 2 different values, the final extrapolation
224 to 0 gives an entropy rate really close to 1 as expected (Figure 1B, right panel).

225 However, when increasing the number of possible values until 256 (entropy H of 8) we start to
226 unravel the so-called “sampling disaster” (Figure 1C). When performing the last extrapolation
227 (Figure 1C, right panel), even if the upper bound has the correct value of 8 (most right point), a
228 linear fit can be done only on the 2 last points and the intersection to 0 gives a value of around
229 5.7, far from the expected one. This is easily explained by the number of data points we have in
230 our model signal. The last extrapolation concerns the “ T ” combinations of values to calculate the
231 entropy rate and when using Gaussian white noise and with T equal to 1, it means we need $2^8 =$
232 256 samples to properly estimate the probability distribution. However, if T increases to 2 we
233 then need $2^{8*2} = 65536$ samples to estimate the probability distribution, when we had only 10000.
234 The probability distribution is thus insufficient to properly estimate the entropy rate of this signal
235 with 256 values. Even by using quadratic extrapolations to compensate for the sampling bias, we
236 can see that the direct method gives a wrong result for high entropy values and few data points
237 (red arrowheads in Figure 1D, left panel).

238 As a comparison, we simply saved the 10 000 samples data of increasing noise as PNG image
239 file with a depth of 8 bits (and thus 256 possible values) and measured the space taken by these
240 files on the hard drive (Figure 1D, right panel). We obtained a linear increase versus the ideal
241 entropy value of equation ($y = 1.199x + 0.609$, $R^2 = 0.99$). The PNG compression algorithm
242 works with linearized data, which means there is no difference when saving pictures as a 100 *
243 100 square format (figure 1D, right panel, squares plot) or saving a 10 000 single line (same

244 [panel, crosses plot](#)). Noticeably, there is no sampling disaster when using this method. From this
245 first test, we can conclude that the size of a PNG file of a model signal has a linear relationship
246 with its entropy rate. And that this measure is not biased by the sampling disaster.

247 As another example to better illustrate the concept of entropy and the effect of PNG conversion,
248 we choose to generate 10 000 points of uniform white noise of amplitude 4 (thus an entropy H of
249 2 bits. [Figure 2A, top left](#)) and compare it to the really same signal, but with sorted values
250 ([Figure 2A, bottom left](#)). These two signals look drastically different but they have the same
251 probability distribution and if we use the Shannon's formula (eq. 1), they both have the same
252 entropy. However, when the signal is sorted the uncertainty of each value is drastically reduced.
253 By knowing any value we have a good guess of what will be the next one, so its entropy should
254 be close to 0. This is exactly what happens when using the quadratic extrapolation to correct the
255 sampling bias: the signal made of uniform white noise keeps its entropy of 2 bits, but the sorted
256 signal sees its entropy reduced to 0.0048 bits per pixel ([Figure 2A, middle](#)). We then multiplied
257 the size of the signal by 2 and 4 (thus 20 000 and 40 000 points): this does not change the
258 probability distribution of the values and thus the entropy values stay low (Entropy of 0.0001 and
259 0.0016 bits per pixel, respectively) ([Figure 2A, middle](#)).

260 The PNG algorithm works by removing statistical redundancy in the signal, but by definition
261 there is no redundancy in a signal made of uniform white noise. As a result, when we increase
262 the size of the random signal by a factor 2 or 4 we increase the size of the corresponding file by
263 the same factor (File sizes of 3.2, 7.1 and 14 kB, respectively) ([Figure 2A, right](#)). If we use the
264 sorted signal, the redundancy is maximal and thus the file size is much smaller, showing the
265 decrease in entropy. If we increase the size of this signal, we increase the redundancy and thus
266 the file size stays low (File sizes of 0.13, 0.12 and 0.16 kB, respectively) ([Figure 2A, right](#)).

267 The entropy of a signal is independent of the mean value of this signal, as it is calculated from a
268 probability distribution of values and not from the values themselves. To demonstrate that the
269 PNG format behaves in the same way, we generated 10 000 points of uniform white noise with 2
270 possible values (0 and 1) and progressively increased the percentage of 1 in this signal, from 0 to
271 100% ([Figure 2B, left](#)). If we calculate the entropy of this signal by the Shannon's formula (eq.1),
272 we obtain the classical bell-shaped curve as described by ([Shannon, 1948](#)) ([Figure 2B, right](#)). We
273 simply saved these signals to PNG format and measured the size of the file on the hard drive, and
274 we could see that this size follows the same curve than the entropy ([Figure 2B, right](#)).

275 From these examples, we conclude that correcting the sampling bias is critical to capture the
276 entropy of a signal. We showed that the PNG conversion method does capture the intrinsic
277 organization of a signal, that it follows its entropy and is independent of the values of the signal
278 itself. However, the different signals need to be of the same size if we want to estimate their
279 entropy by PNG conversion.

280 2 Mutual Information and application to electrophysiological data

281 Most of the time, the experimenter is not interested in the entropy itself, but in the mutual
282 information between two variables X and Y. The mutual information “ I_{XY} ” measures the
283 statistical dependence by the distance to the independent situation (Cover and Thomas, 2006;
284 Shannon, 1948) given by

$$285 \quad I_{XY} = \sum_{i,j} p(x_i, y_j) \log_2 \left(\frac{p(x_i, y_j)}{p(x_i)p(y_j)} \right) \quad (\text{eq.3})$$

286 Therefore, when X and Y are independent $p(x_i, y_j) = p(x_i) * p(y_j)$, so $I_{XY} = 0$ bits.

287 The mutual information can also be rewritten as the difference between the entropy of X and the
288 conditional entropy of X given Y:

$$289 \quad I_{XY} = H(X) - H(X/Y) \quad (\text{eq.4})$$

290 Where $H(X)$ is the entropy already described (eq.1) and

$$291 \quad H(X/Y) = - \sum_j p(y_j) \sum_i p(x_i, y_j) * \log_2 p(x_i, y_j) \quad (\text{eq.5})$$

292 Interestingly, if we consider a neuron stimulated repetitively by the same stimulus, we can define
293 X as the response of the neuron to the stimulus and Y as the stimulus received by the neuron
294 (Borst and Theunissen, 1999). In that case, $H(X)$ can be interpreted as the total entropy
295 (quantifying the average variability of the neuron response during one trial), also called H_S .
296 $H(X/Y)$ can be interpreted as the noise entropy H_N , quantifying the variability of the neuron
297 response across the trials. In that case,

$$298 \quad I_{SN} = H_S - H_N \quad (\text{eq.6})$$

299 Where H_S is the average entropy of every trial and:

$$300 \quad H_N = - \langle \sum_i p(x_i)_\tau * \log_2 p(x_i)_\tau \rangle_\tau \quad (\text{eq.7})$$

301 where $p(x_i)_\tau$ is the probability of finding the configuration x_i at a time τ over all the acquired
302 trials of an experiment (Juusola and de Polavieja, 2003; de Polavieja et al., 2005; Strong et al.,
303 1998). Finally, we can obtain the information rate R, by using the quadratic extrapolation method
304 and dividing by the time sampling, as:

$$305 \quad R = R_S - R_N = \lim_{T \rightarrow \infty} \frac{1}{T} \lim_{v \rightarrow \infty} \lim_{Size \rightarrow \infty} (H_S^{T,v,Size} - H_N^{T,v,Size}) \quad (\text{eq.8})$$

306 In practical terms, this means to acquire multiple recordings of the same experiments, apply the
307 quadratic extrapolation method first on each trial and average the results to obtain R_S . Then, to

308 apply the same method across the trials for every time τ and average the results to obtain R_N . The
309 information rate R is thus the mutual information between the stimulation protocol and the
310 acquired trials.

311 In order to apply this method to electrophysiological signals, we created a single compartment
312 model in NEURON 7.7. The model was stimulated using various numbers of EPSPs with
313 amplitudes chosen randomly in a log-normal distribution described in (Lefort et al., 2009). Each
314 synapse stimulated the model once during a simulation and the time onset was randomly chosen.
315 We ran 20 trials of the simulation with the same train of synapses (Figure 3A, left). In order to
316 introduce some randomness in the spiking, a small Gaussian noise current was also injected
317 (Figure 3A, left, See Methods). We calculated R_S and R_N using the quadratic extrapolation
318 method. (Figure 3A, middle) and subtracting R_N to R_S to obtain the information rate (Figure 3A,
319 right). We then reproduced this protocol with increasing numbers of synapses to obtain different
320 spiking frequencies. As expected, when we increased the number of synapses we increased the
321 spiking frequency and the mutual information between our stimulation and the response (Figure
322 3A, right). This measure follows a linear trend, really similar to what was already described in
323 literature (Juusola and de Polavieja, 2003; de Polavieja et al., 2005).

324 As already described, the PNG format is line-wise. The compression algorithm will thus be
325 sensitive to the orientation of the image we have to compress. To estimate the entropy of the
326 signal, we started by converting our voltage signals to an 8-bits PNG image (256 levels of grey).
327 As our signals are 20 trials of 5s at 10 kHz sampling, this yielded a 50 000 * 20 pixels of 256
328 grey scale image (Figure 3B, left). We saved this first version of the image and measured the size
329 of the files on the hard drive. To estimate the entropy of the noise, we simply rotated the image
330 90 degrees and saved it again to PNG format. This constrains the algorithm to calculate the
331 entropy through the acquired trials and not through the signal itself, thus estimating the entropy
332 of the noise through every trials (Figure 3B, middle). We measured the size of the newly
333 generated file and subtracted it to the previously measured for the signal entropy. As we can see,
334 this difference of file size follows a linear behavior, increasing with AP frequency similarly to
335 the direct measure of the information rate (Figure 3B, right).

336 As a second example, we reproduced the protocol made by (London et al., 2002) to estimate the
337 information transfer between one synapse and the postsynaptic neuron. We stimulated the model
338 with 750 of the synapses described above to get a spiking frequency around 5Hz and added a
339 supplementary synapse stimulating the model every 200 ms. The EPSP size of this synapse
340 (wSyn_supp) was modified at each simulation. When wSyn_supp was weak, this synapse did not
341 drive the spiking of the model (Figure 3C, up left). When wSyn_supp was strong, this synapse
342 drove the spiking of the model (Figure 3C, down left). We made 100 trials for each wSyn_supp
343 and at each trial the onset time and amplitude of the others synapses were chosen randomly. We
344 down-sampled our signal to 3 kHz and binarized it to 0 and 1, depending on the presence of APs
345 or not similarly to (London et al., 2002). After calculating the Information rate using the
346 quadratic extrapolation method, we obtained a sigmoid curve similar to what they described

347 (London et al., 2002) (Figure 3C, middle). In a similar way than above, we converted our voltage
348 signals to a 1-bit PNG image (2 levels of grey). As our signals are 100 trials of 5s at 3 kHz
349 sampling, this yielded an image of 15 000 * 100 pixels of 2 possible values. We measured the
350 size of the file, then rotated the image 90 degrees, saved it again and measured the size of this
351 new file. As expected, the difference between the sizes of these two files follows a sigmoid curve
352 really similar to the one calculated by the quadratic extrapolation method (Figure 3C, right).

353 From this second test, we conclude that by saving multiple trials of the same experiment as a
354 single PNG file, we can estimate the entropy of the signal. And by simply rotating this same file
355 90 degrees and saving it again, we can estimate the entropy of the noise. The difference between
356 those two values follows the same behavior than measuring the Mutual Information between the
357 stimulation protocol and the multiple recorded responses.

358 **3 Application to 2D images**

359 Another way to understand entropy is that it is a representation of complexity of a signal (Cover
360 and Thomas, 2006). For example, (Wagstaff and Corsetti, 2010) used the PNG compression
361 algorithm to evaluate the complexity of biogenic and abiogenic stromatolites. As a quick
362 example, we took one of the famous drawings of a cortical column by Santiago Ramon y Cajal
363 (Cajal, 1899) (Figure 4A, top, Wikimedia Commons). We saved each 1-pixel column of this
364 picture as an 8-bits PNG file and measured its size on the hard drive. As we see, the size of the
365 columns as PNG files changes with the different layers of the cortical stack, illustrating the
366 differences in cell density and dendrites arborizations (Figure 4A, bottom).

367 In the same spirit, we used the ddAC Neuron example from the FIJI distribution of the ImageJ
368 software (Schindelin et al., 2012). This reconstructed drosophila neuron (Figure 4Ba) is a classic
369 example used for Sholl analysis (Ferreira et al., 2014; Sholl, 1953), (see
370 https://imagej.net/Sholl_Analysis). This analysis estimates the complexity of an arborization by
371 drawing concentric circles centered on the soma of the neuron and counting the number of
372 intersections between those circles and the dendrites. The more intersections, the more complex
373 is the dendritic tree. As we need PNG files with the same dimensions to be able to compare their
374 sizes, we realized a cylindrical anamorphosis centered on the soma of the ddAC neuron (Figure
375 3Bb) and saved each column of this new rectangular image as PNG files. As a result, the size of
376 those files grew with the distance from soma, reaching the same peak than a Sholl analysis made
377 with default settings in Fiji (Figure 4Bc). Of course, it is also possible to simply tile the original
378 image in smaller PNG files and save them independently. The size of these files will give an idea
379 of the complexity of the area covered by the tile (Figure 4Bd).

380 In a final example, we used a group of images made by Dieter Brandner and Ginger Withers
381 available in the Cell Image Library (<http://cellimagelibrary.org/groups/3006>). These images are
382 under Creative Common Attribution Licence and show the growth of neuronal cultures from 2 to
383 7 days In-Vitro. They show two stainings, for tubulin and MAP2. They are suitable to our needs

384 as all the images have the same dimensions and resolution. We kept only the MAP2 channel as it
385 reveals the dendrite morphology, converted the images to 8-bits grey scale (256 grey levels) and
386 thresholded them to remove the background (Figure 4C, left and middle). We then saved all the
387 images to PNG, measured the size of the files on the hard drive and divided this number by the
388 number of visible somas, in order to make a quick normalization by the culture density. As
389 expected, this ratio File Size / Number of Cells increases with the number of days in culture,
390 revealing the dendrite growth (Figure 4C, right).

391 From this third test, we showed that we can use the PNG format to estimate the entropy of 2D
392 images as well, and this can be used to estimate dendrite growth or local complexity of an image.

393 **4 Discussion**

394 Entropy measurement can be a tool of choice in neuroscience, as it applies to many different
395 types of data; it can capture nonlinear interactions, and is model independent. However, an
396 accurate measure can be difficult as it is prone to a sampling bias depending of the size of the
397 recorded signal, its quantization levels and its sampling. There are multiple ways to compensate
398 for it, but none them trivial. In this paper, we showed that it is possible to estimate the entropy
399 rate of neuroscience data simply by compressing them in PNG format and measuring the size of
400 the file on the hard drive. The principle relies on the Source Coding Theorem specifying that one
401 cannot compress a signal more than its entropy multiplied by its size. We showed first that the
402 size of PNG files correlates linearly with the entropy of signals made of Uniform white noise.
403 Then that we can estimate the information transfer rate between a stimulation protocol and the
404 measured response simply by saving the responses as a PNG file, measuring the size and
405 subtracting the size of the same file rotated 90 degrees. And finally, that we can generally use the
406 PNG format to estimate complexity of two-dimensional data like neuronal arborization and in
407 histological stainings.

408 **1 Drawbacks**

409 The main drawback of this method is that the PNG file size is not the absolute value of the
410 entropy of the signal. Even if entropy bits and computer bytes do share similar names, in no
411 cases should we exchange one for the other. A PNG file size is a way to estimate the evolution of
412 entropy, considering all other parameters unchanged. As so, PNG files must be all of the same
413 dimensions, of the same dynamic range and saved with the same software. A PNG file is
414 composed of a header, critical chunks and non-essential ancillary chunks (See Methods).
415 Different software will save different data in the ancillary chunks and thus will change the size of
416 the file, independently of the compressed signal.

417 **2 Advantages**

418 The main advantage of this method is that it relies on previously developed compression
419 algorithms that were already shown as optimal (Huffman, 1952). Moreover, it does not need any
420 specialized software or any knowledge in programming language, as the PNG format is
421 ubiquitous in informatics. For example, the ImageJ software is widely used in neuroscience and
422 can export data as PNG.

423 A second advantage is the speed of execution. As an example, the Information Rate of neuronal
424 signals (Figure 3A & B) took a bit more than 2 hours of calculation for the quadratic
425 extrapolation method. Saving the same signals in PNG took less than 30 seconds.

426 As so, this method is extremely easy, quick, and does not need any knowledge in mathematics
427 for correcting the sampling bias. It is interesting to note that an experimenter will often acquire
428 multiple recordings of the same protocol in order to infer proper statistics. This means that most
429 of the times no supplementary experiments are needed to calculate the entropy of a signal, or the
430 information transfer rate between a stimulation protocol and its recorded result.

431 In conclusion, we propose this method as a quick-and-easy way to estimate the entropy of a
432 signal or the information transfer rate between stimulation and recorded signals. It does not give
433 the exact value of entropy or information, but it is related to it in a linear way and its evolution
434 through different parameters follows a linear trend as well. And it is not affected by the sampling
435 bias inherent to the direct way of calculating entropy.

436 **3 Developments**

437 We see multiple ways to improve this method. First, we saved our data as 8-bits PNG files,
438 which limits the dynamic range of the file to 256 values. However, it is possible to save PNG
439 natively as 1, 4, 8, 16 and 24 bits range, thus greatly increasing the dynamic range of the saved
440 signal. Second, with some programming skills it is possible to remove the header and ancillary
441 chunks of the PNG format, thus removing the size overhead (but the file will be unreadable by
442 standard softwares). Finally, one possible way of improving the estimation of entropy rate would
443 be to choose a better compression algorithm. We choose the PNG format as it is widely used by
444 common softwares and it is based on LZSS and Huffman algorithms, which have been proven
445 optimal. However, some algorithms may give a better compression rate depending on the quality
446 of the data. As an example, the Rice compression algorithm was originally developed for the
447 NASA Voyager missions (Rice and Plaunt, 1971). It is suboptimal but is better suited for noisy
448 signals of low values.

449 In a more general direction, it is important to note that this method works with any entropy-
450 coding compression algorithm, as long as they are loss-less. This is the case of GZip algorithms
451 for example, used in many compression softwares such as WinRAR, PKZIP, ARJ, etc... It is

452 thus not limited to pictures in PNG, although this format is useful for rotating the file and
453 estimating the mutual information easily. Moreover, we apply these algorithms to 2D images,
454 when actually the algorithm linearizes the data and works only in linear way on one dimension.
455 There are some attempts to generalize Shannon entropy to 2D space (Larkin, 2016), but they are
456 out of the scope of this paper.

457 **5 References**

- 458 Bialek, W., Rieke, F., Steveninck, R. de R. van, and Warland, D. (1991). Reading a neural code.
459 *Science* 252, 1854–1857.
- 460 Bian, N., Liang, F., Fu, H., and Lei, B. (2019). A Deep Image Compression Framework for Face
461 Recognition. ArXiv190701714 Cs.
- 462 Borst, A., and Theunissen, F.E. (1999). Information theory and neural coding. *Nat. Neurosci.* 2,
463 947–957.
- 464 Cajal, S.R. (1899). Comparative study of the sensory areas of the human cortex.
- 465 Cover, T., and Thomas, J. (2006). *Elements of Information Theory*, 2nd Edition | Wiley.
- 466 Deutsch, P. (1996). DEFLATE Compressed Data Format Specification version 1.3.
- 467 Ferreira, T.A., Blackman, A.V., Oyrer, J., Jayabal, S., Chung, A.J., Watt, A.J., Sjöström, P.J.,
468 and van Meyel, D.J. (2014). Neuronal morphometry directly from bitmap images. *Nat. Methods*
469 11, 982–984.
- 470 Hou, Y., Zheng, L., and Gould, S. (2020). Learning to Structure an Image with Few Colors.
471 ArXiv200307848 Cs.
- 472 Hu, W., Tian, C., Li, T., Yang, M., Hou, H., and Shu, Y. (2009). Distinct contributions of Nav1.6
473 and Nav1.2 in action potential initiation and backpropagation. *Nat. Neurosci.* 12, 996–1002.
- 474 Huffman, D.A. (1952). A Method for the Construction of Minimum-Redundancy Codes. *Proc.*
475 *IRE* 40, 1098–1101.
- 476 Ince, R.A.A., Giordano, B.L., Kayser, C., Rousset, G.A., Gross, J., and Schyns, P.G. (2017). A
477 statistical framework for neuroimaging data analysis based on mutual information estimated via
478 a gaussian copula. *Hum. Brain Mapp.* 38, 1541–1573.
- 479 Ito, S., Hansen, M.E., Heiland, R., Lumsdaine, A., Litke, A.M., and Beggs, J.M. (2011).
480 Extending Transfer Entropy Improves Identification of Effective Connectivity in a Spiking
481 Cortical Network Model. *PLoS ONE* 6.
- 482 Juusola, M., and de Polavieja, G.G. (2003). The rate of information transfer of naturalistic
483 stimulation by graded potentials. *J. Gen. Physiol.* 122, 191–206.

- 484 Larkin, K.G. (2016). Reflections on Shannon Information: In search of a natural information-
485 entropy for images. ArXiv160901117 Cs Math.
- 486 Larsson, N.J. (1996). Extended Application of Suffix Trees to Data Compression. In In Data
487 Compression Conference, pp. 190–199.
- 488 Larsson, N.J. (1999). Structures of String Matching and Data Compression. thesis/docmono.
489 Lund University.
- 490 Lefort, S., Tomm, C., Floyd Sarria, J.-C., and Petersen, C.C.H. (2009). The excitatory neuronal
491 network of the C2 barrel column in mouse primary somatosensory cortex. *Neuron* 61, 301–316.
- 492 London, M., Schreibman, A., Häusser, M., Larkum, M.E., and Segev, I. (2002). The information
493 efficacy of a synapse. *Nat. Neurosci.* 5, 332–340.
- 494 Magri, C., Whittingstall, K., Singh, V., Logothetis, N.K., and Panzeri, S. (2009). A toolbox for
495 the fast information analysis of multiple-site LFP, EEG and spike train recordings. *BMC*
496 *Neurosci.* 10, 81.
- 497 Mentzer, F., Van Gool, L., and Tschannen, M. (2020). Learning Better Lossless Compression
498 Using Lossy Compression. ArXiv200310184 Cs Eess.
- 499 Nemenman, I., Bialek, W., and de Ruyter van Steveninck, R. (2004). Entropy and information in
500 neural spike trains: progress on the sampling problem. *Phys. Rev. E Stat. Nonlin. Soft Matter*
501 *Phys.* 69, 056111.
- 502 Paninski, L. (2003). Convergence properties of three spike-triggered analysis techniques. *Netw.*
503 *Bristol Engl.* 14, 437–464.
- 504 Panzeri, S., and Treves, A. (1996). Analytical estimates of limited sampling biases in different
505 information measures. *Netw. Bristol Engl.* 7, 87–107.
- 506 Panzeri, S., Senatore, R., Montemurro, M.A., and Petersen, R.S. (2007). Correcting for the
507 sampling bias problem in spike train information measures. *J. Neurophysiol.* 98, 1064–1072.
- 508 de Polavieja, G.G., Harsch, A., Kleppe, I., Robinson, H.P.C., and Juusola, M. (2005). Stimulus
509 history reliably shapes action potential waveforms of cortical neurons. *J. Neurosci. Off. J. Soc.*
510 *Neurosci.* 25, 5657–5665.
- 511 Rice, R., and Plaunt, J. (1971). Adaptive Variable-Length Coding for Efficient Compression of
512 Spacecraft Television Data. *IEEE Trans. Commun. Technol.* 19, 889–897.
- 513 Rueden, C.T., Schindelin, J., Hiner, M.C., DeZonia, B.E., Walter, A.E., Arena, E.T., and Eliceiri,
514 K.W. (2017). ImageJ2: ImageJ for the next generation of scientific image data. *BMC*
515 *Bioinformatics* 18, 529.
- 516 Safaai, H., Onken, A., Harvey, C.D., and Panzeri, S. (2018). Information estimation using
517 nonparametric copulas. *Phys. Rev. E* 98.

- 518 Schindelin, J., Arganda-Carreras, I., Frise, E., Kaynig, V., Longair, M., Pietzsch, T., Preibisch, S.,
519 Rueden, C., Saalfeld, S., Schmid, B., et al. (2012). Fiji: an open-source platform for biological-
520 image analysis. *Nat. Methods* 9, 676–682.
- 521 Shannon, C.E. (1948). A Mathematical Theory of Communication. *Bell Syst. Tech. J.* 27, 379–
522 423.
- 523 Sholl, D.A. (1953). Dendritic organization in the neurons of the visual and motor cortices of the
524 cat. *J. Anat.* 87, 387–406.
- 525 Storer, J.A., and Szymanski, T.G. (1982). Data compression via textual substitution. *J. ACM* 29,
526 928–951.
- 527 Street, S. (2020). Upper Limit on the Thermodynamic Information Content of an Action
528 Potential. *Front. Comput. Neurosci.* 14, 37.
- 529 Strong, S.P., Koberle, R., de Ruyter van Steveninck, R.R., and Bialek, W. (1998). Entropy and
530 Information in Neural Spike Trains. *Phys. Rev. Lett.* 80, 197–200.
- 531 Timme, N.M., and Lapish, C. (2018). A Tutorial for Information Theory in Neuroscience.
532 *ENeuro* 5.
- 533 Vicente, R., Wibral, M., Lindner, M., and Pipa, G. (2011). Transfer entropy—a model-free
534 measure of effective connectivity for the neurosciences. *J. Comput. Neurosci.* 30, 45–67.
- 535 Wagstaff, K.L., and Corsetti, F.A. (2010). An evaluation of information-theoretic methods for
536 detecting structural microbial biosignatures. *Astrobiology* 10, 363–379.
- 537 Wiegand, T. (2010). Source Coding: Part I of Fundamentals of Source and Video Coding. *Found.*
538 *Trends® Signal Process.* 4, 1–222.

539

540 **6 Funding**

541 This work was funded by Marie-Curie Fellowship IF-746247 Astromodulation, by the Wellcome
542 Trust Principal Fellowship (212251/Z/18/Z), and by the ERC Proof of Principle grant (767372 –
543 NEUROCLOUD).

544 **7 Acknowledgements**

545 We thank Q. Bernard, C. Leterrier, V. Marra, T. Jensen, K. Zheng for helpful discussion.

546

547 **Figure Legends**

548 **1 Figure 1: comparison of entropy and PNG file size on a model case.**

549 A) Examples of 10 000 data points of uniform white noise with growing number of grey levels
550 and growing entropy (here showed as square picture signals). Left: 2 possible grey values, or
551 entropy of 1. Right: 256 possible grey values, or entropy of 8.

552 B) Direct calculation and quadratic extrapolations to 0 to calculate the entropy rate of the left
553 signal in A). Left: Plotting all the entropy values to $1/\text{Size}$ and extrapolating to 0 to get the value
554 for infinite size (white arrowhead). For clarity, only the condition for $v = 2$ is shown. Middle:
555 plotting the obtained values at left to $1/v$ and extrapolating to 0 to get the value for infinite
556 number of binning (white arrowhead). Right: plotting the final values to $1/T$ and extrapolating to
557 0 to get the value for infinite number of combinations of letters (black arrowhead). Note that this
558 value is really close to 1, as expected when using a signal made of uniform white noise with 2
559 possible values.

560 C) Direct calculation and quadratic extrapolations to 0 to calculate the entropy rate of the right
561 signal in A). Left: Only the condition for $v = 2$ is shown. Note that in the final graph (right),
562 points do not follow a linear trend. When using the last 2 points for extrapolation to 0, the value
563 is far from the expected value of 8 (red arrowhead).

564 D) Left: when plotted against the known entropy value, the quadratic extrapolation method
565 shows examples of sampling disaster for high values of entropy (red arrowheads). Right: when
566 simply saving all the signals described in A), the file size in kBytes shows a linear relationship
567 with the signal entropy ($y = 1.199x + 0.609$, $R^2 = 0.99$). Not that this true for pictures made
568 either of square signals (squares plot) or linearized signals (crosses plot) and there is no sampling
569 disaster with this method.

570 **2 Figure 2: Effect of redundancy and signal size on entropy and PNG file** 571 **size.**

572 A) Left, Top: Example of 10 000 data points of uniform white noise with 4 levels (entropy of 2
573 bits, here showed as square picture signals). Left, Bottom: the same signal, with sorted values. If
574 we use the Shannons's formula for calculating entropy, both signals have an entropy of 2 bits.
575 Middle: Effect of sampling bias correction and size of the signal on the entropy value. With the
576 Shannon's formula, both random and sorted signals have the same entropy value (crosses plot).
577 If we correct the sampling bias with the quadratic extrapolation method, the entropy of the sorted
578 signal decreases dramatically (squares plot). In both cases, changing the size of the signal does
579 not change the entropy value, as it does not change the probability distribution of each value in
580 the signal. Right: As the PNG algorithm compresses by removing statistical redundancy in the
581 signal, the file size will grow with the size of the random signal. A sorted signal has a maximal
582 redundancy and thus its file size will stay almost constant when increasing the signal size.

583 **B)** Left: Example of multiple signals of 10 000 data points (here showed as square picture signals)
584 with 2 possible grey levels (or 0 and 1) and a growing percentage of white (or 1). Right: Direct
585 entropy calculation of these signals (grey dashed line) and normalized PNG file size as a
586 comparison (black line).

587 **3 Figure 3: Comparison of information rate and PNG file size on a** 588 **neuronal model.**

589 **A)** Left: example of 20 generated trials with the same synaptic activity. Due to the injection of a
590 small Gaussian noise current, we obtain variability in the spiking of the different trials. Arrows
591 show the direction used with the quadratic extrapolation method to calculate the signal entropy
592 (R_S) and noise entropy (R_N). Middle: calculation of the Entropy Rate of the Signal (R_S) and the
593 noise (R_n) for the full voltage of the cell for each condition. The Information transfer Rate R is
594 the difference between R_S and R_n . Right: Information transfer Rate between the synaptic
595 stimulation and the neuronal activity, versus the spiking frequency. This follows a linear trend
596 ($y = 25.935 x + 188.15$, $R^2 = 0.97$).

597 **B)** Left: Conversion of the modeled trials in A) as a 256 grey values PNG file. As the PNG
598 conversion algorithm is line-wise, we have to save the image a first time, then rotate it 90
599 degrees and save it a second time (Middle). Arrows show the direction of compression. Right:
600 the subtraction of the 2 images sizes follows a linear trend with the spiking frequency ($y =$
601 $2.555 x - 4.12$, $R^2 = 0.98$).

602 **C)** Left: examples of rastergrams showing the impact of the supplementary synapse on our
603 neuronal model. With a low synaptic strength ($w_{Syn_supp} = 2$ mV, top), this synapse barely
604 drives the model. With a high synaptic strength ($w_{Syn_supp} = 6$, bottom), the neuron spiking
605 starts to synchronize with the occurrence of the synapse. Middle: Information transfer Rate
606 between the activity of the supplementary synapse and the neuronal spiking. As expected, it
607 follows a sigmoidal behavior. Right: rastergrams were saved as PNG files, rotated 90 degrees
608 and saved again. The difference of the 2 files sizes follows a similar curve than the Information
609 transfer Rate.

610 **4 Figure 4: Application to 2D data.**

611 **A)** Top: original drawing of a cortical column by Santiago Ramon y Cajal. Arrow: each column
612 of pixel was saved as a PNG file. Bottom: File size of each column as PNG, revealing the change
613 in organization and complexity of the different layers.

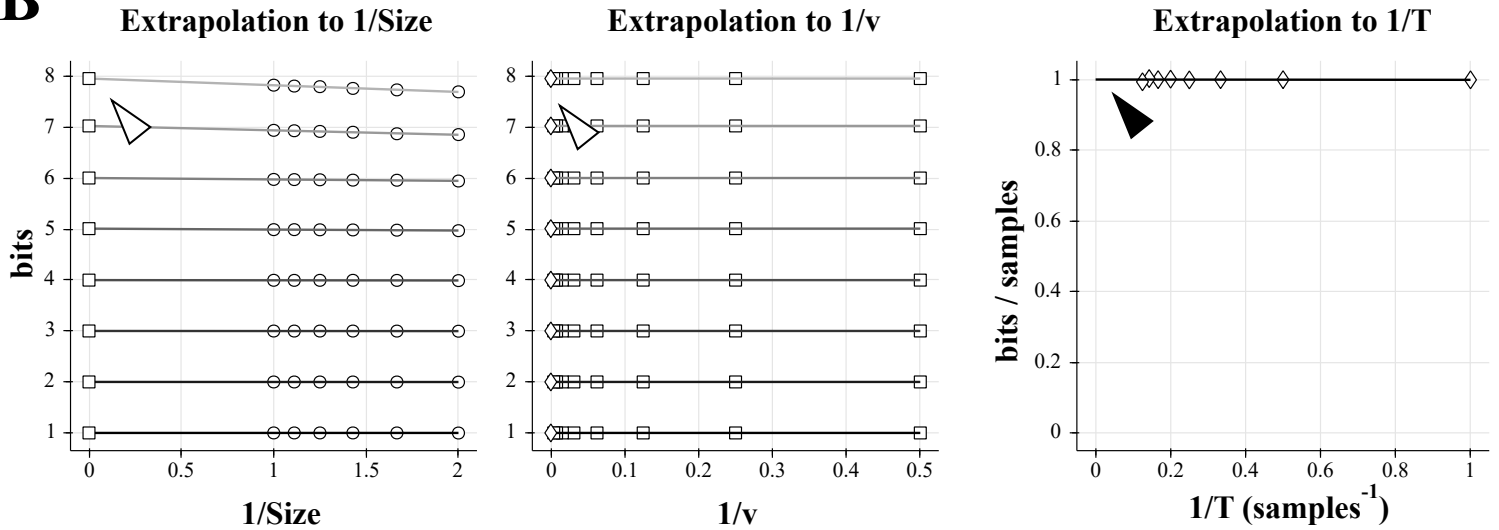
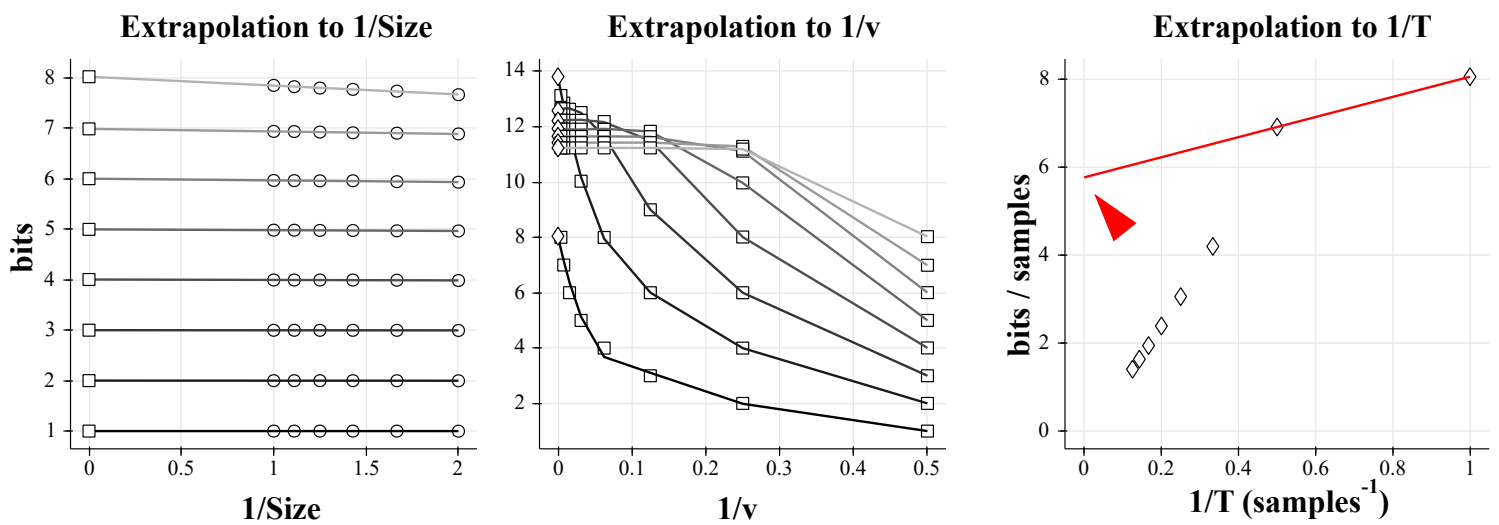
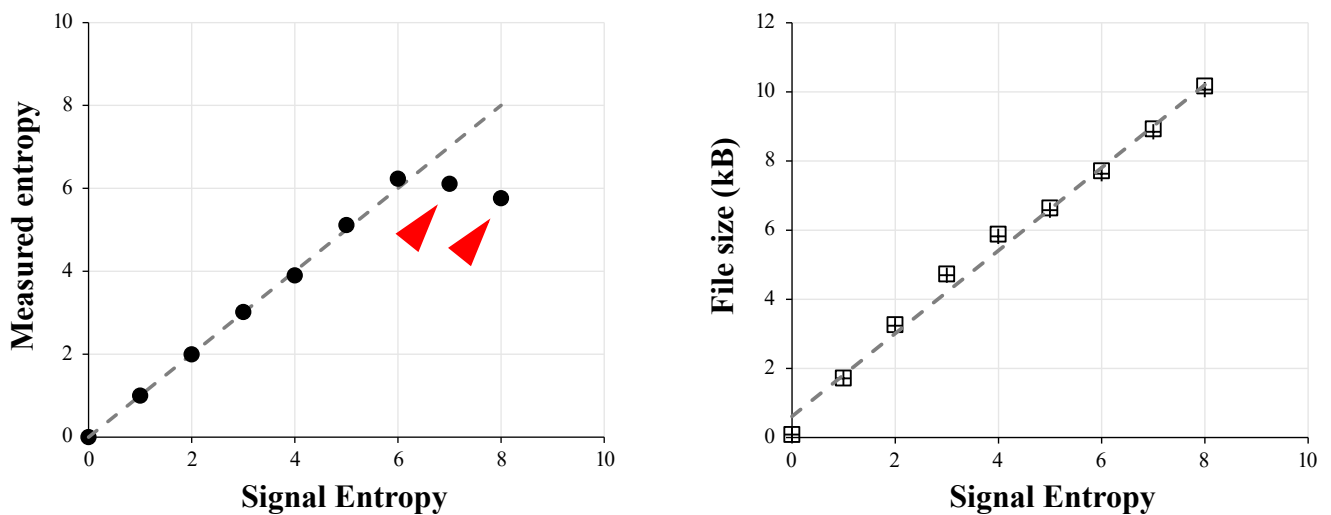
614 **B)** a: ddAC Neuron from Fiji examples. b: The same neuron after a circular anamorphosis
615 centered on the soma. Note how the complexity of the dendritic arbor changes versus distance
616 from soma. Arrow: each column of pixel was saved as a single PNG file. c: file size of these
617 columns as PNG, showing the growth in complexity of the dendritic arborization (black line). As
618 a comparison, we performed a Sholl analysis of the same image with default FIJI parameters

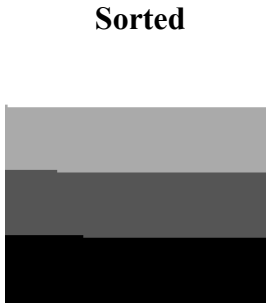
619 (grey line). d: the original image was tiled in 10 squares, and each square saved as a PNG file.
620 The sizes of these files reveal the heterogeneity of the dendritic arborization.

621 **C)** Left and Middle: examples of MAP2 stainings of Brandner and Withers neuronal cultures at 2
622 and 7 Days In Vitro. Note the growth in dendritic arborization through time. Right: Each image
623 was saved into a PNG file, and the file size divided by the number of visible somas. This gives
624 us a file size normalized by the density of the culture. This value increases with the number of
625 Days In-Vitro, revealing the dendrite growth.

A**H = 1 (2 grey values)****H = 8 (256 grey values)**

<https://doi.org/10.1101/2020.08.04.236174>; this version posted August 5, 2020. The copyright holder for this preprint (which was not certified by peer review) is the author/funder, who has granted bioRxiv a license to display the preprint in perpetuity. It is made available under aCC-BY-NC 4.0 International license.

B**C****D**

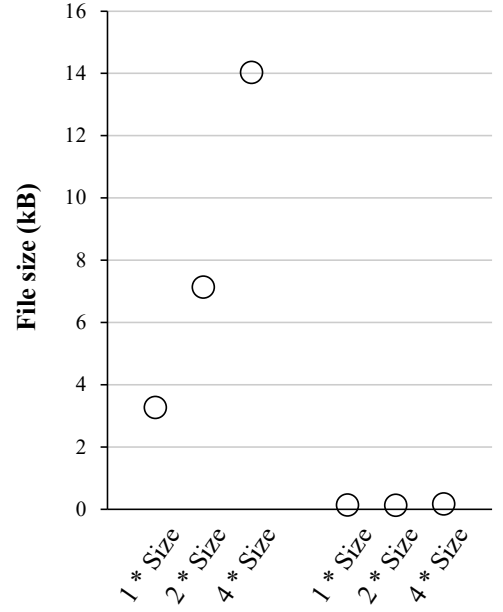
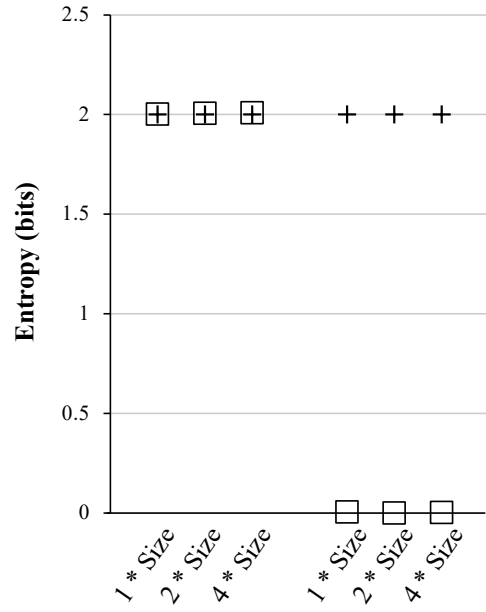
A**H = 2 (4 grey values)**

+ Shannon's Formula

□ Correction by quadratic extrapolation

○ PNG conversion

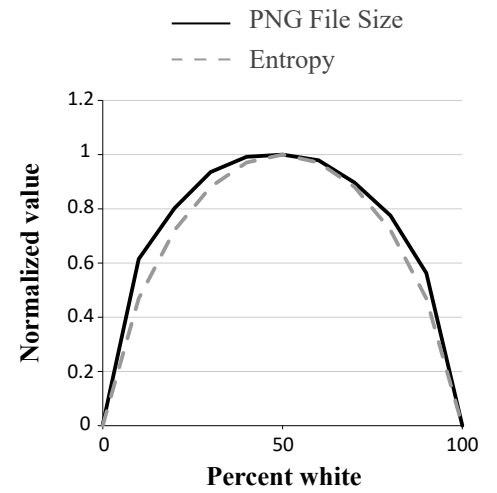
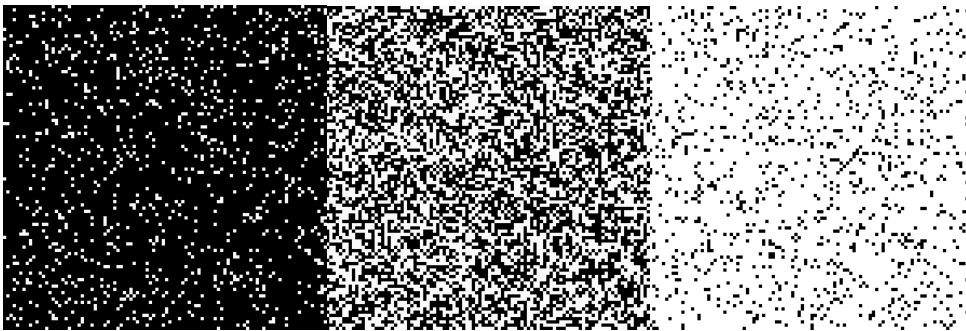
bioRxiv preprint doi: <https://doi.org/10.1101/2020.08.04.236174>; this version posted August 5, 2020. The copyright holder for this preprint (which was not certified by peer review) is the author/funder, who has granted bioRxiv a license to display the preprint in perpetuity. It is made available under aCC-BY-NC 4.0 International license.

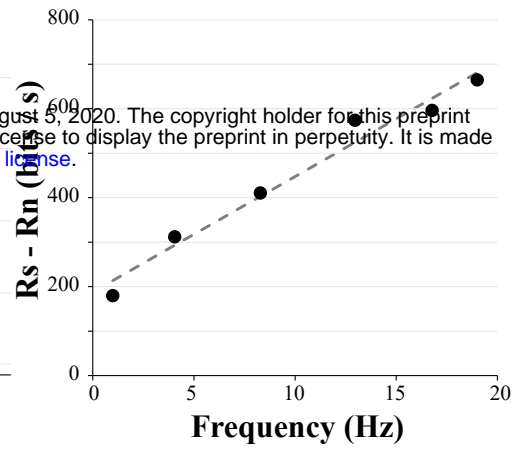
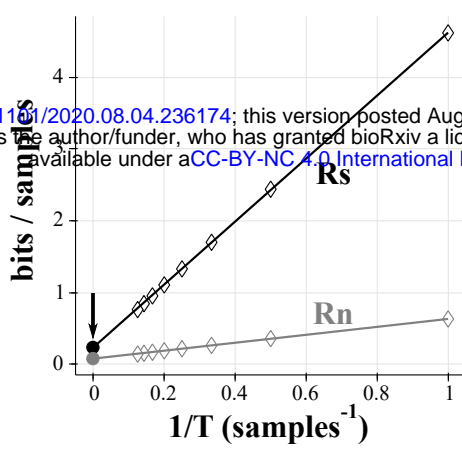
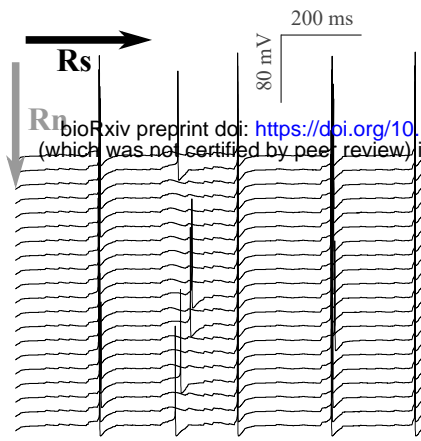
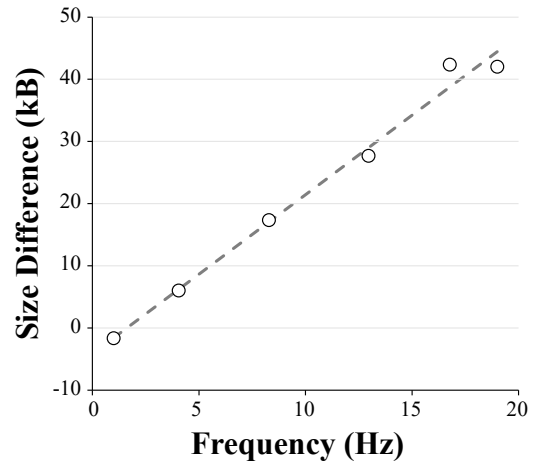
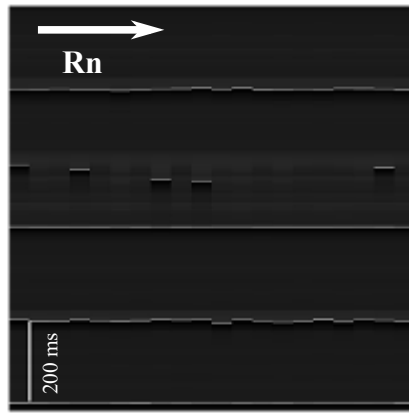
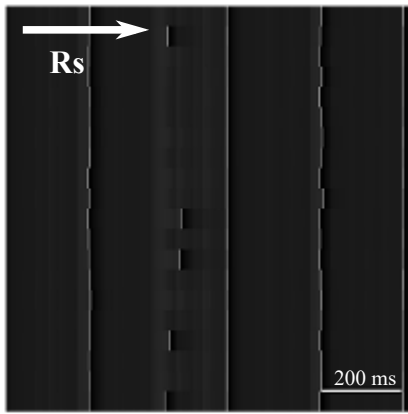
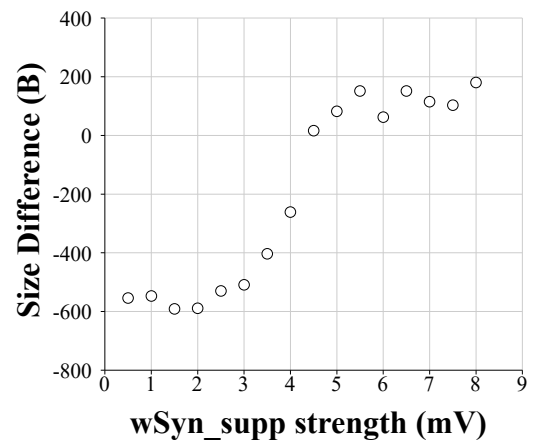
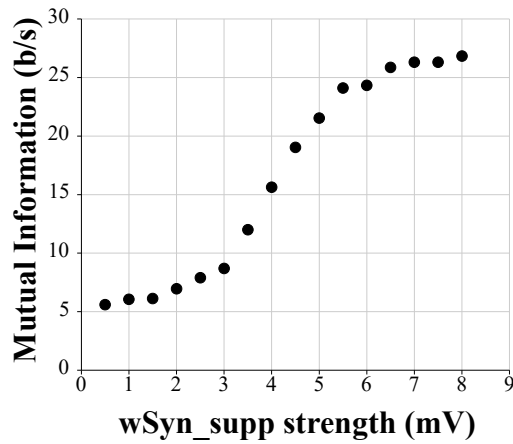
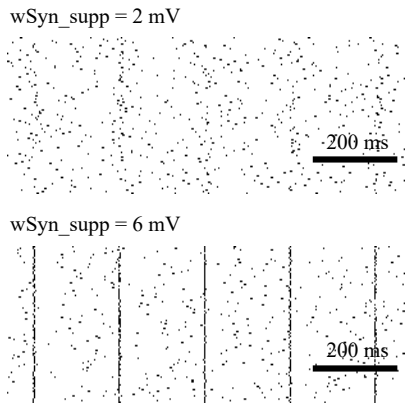
**B****Percent of white values**

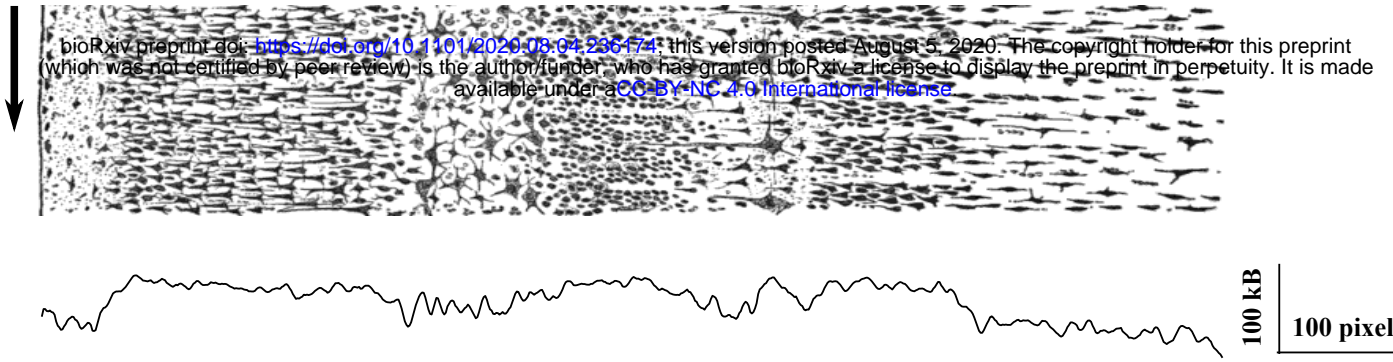
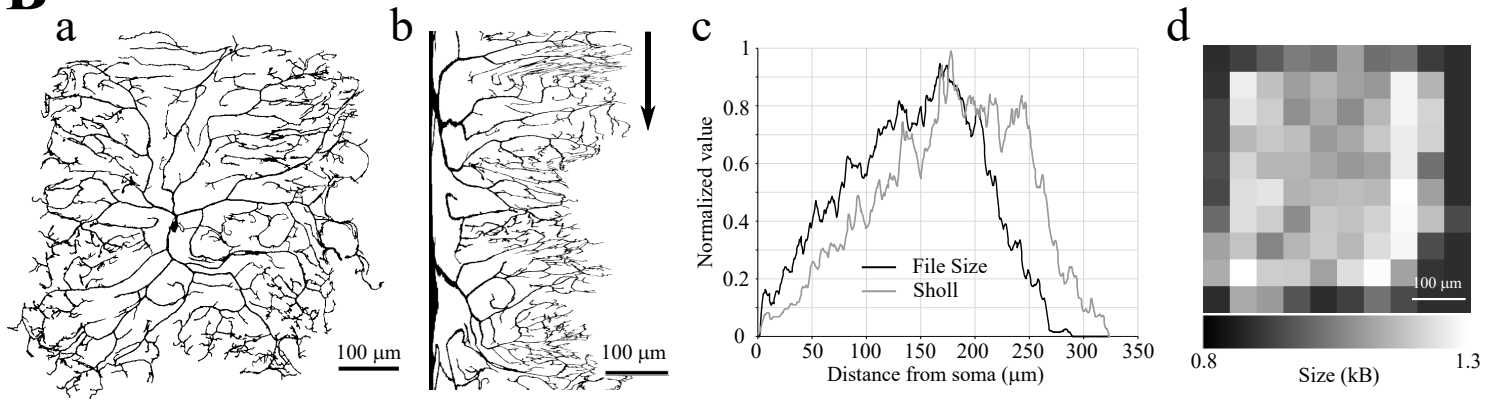
10 %

50 %

90 %



A**B****C**

A**B****C**